Transcriptional analysis of a major capsid protein gene from Spodoptera exigua ascovirus 5a

Article *in* Archives of Virology · February 2008

DOI: 10.1007/s00705-007-1081-3 · Source: PubMed

6 authors, including:

Tamer Salem
Zewail University of Science and Technology
47 PUBLICATIONS **387** CITATIONS
SEE PROFILE

Jian-Li Xue
Mississippi State University
11 PUBLICATIONS **170** CITATIONS
SEE PROFILE

Xiu-Feng Wan
Mississippi State University
181 PUBLICATIONS **2,823** CITATIONS
SEE PROFILE

Xiao-Wen Cheng
Miami University
65 PUBLICATIONS **823** CITATIONS
SEE PROFILE

Arch Virol (2008) 153: 149–162
DOI 10.1007/s00705-007-1081-3
Printed in The Netherlands

Archives of Virology

Transcriptional analysis of a major capsid protein gene from Spodoptera exigua ascovirus 5a

T. Z. Salem*, **C. M. Turney**, **L. Wang****, **J. Xue**, **X.-F. Wan*****, **X.-W. Cheng**

Department of Microbiology, Miami University, Oxford, OH, U.S.A.

Received 9 August 2007; Accepted 17 September 2007; Published online 5 November 2007

Summary

The major capsid protein (*mcp*) gene of Spodoptera exigua ascovirus 5a (SeAV-5a) was confirmed by aphidicolin viral DNA replication inhibition analysis to be a late gene. The 5′ and 3′ ends of *mcp* gene transcripts have been mapped. Primer extension analyses indicated that transcription of the *mcp* gene initiates from a cytosine 25 nucleotides (nt) upstream of the translation start codon. Two independent approaches by 3′ rapid amplification of cDNA ends (3′ RACE) and oligo (dT) cellulose binding assay suggested that SeAV-5a *mcp* mRNA is polyadenylated. Analyses by 3′ RACE also revealed that *mcp* transcripts terminate at a U, either at 26 or 38 nt downstream of the translation stop codon. The putative 5′ transcription control region of the SeAV-5a *mcp* gene shares similarities with other ascoviruses and Chilo iridescent virus (CIV), containing a conserved TATA-box-like motif (TAATTAAA) and an ATTTGATCTT motif upstream of it. The 3′ downstream regions of the *mcp* gene of all the ascoviruses examined and CIV can form a stem-loop structure, and the ends of the *mcp* gene transcripts of SeAV-5a are within the predicted stem-loop region. This suggests that the stem-loop structure of the *mcp* gene might be involved in transcription termination.

Introduction

Among viruses infecting insects, ascoviruses form a new family, *Ascoviridae*, which was only recently recognized by the International Committee on the Taxonomy of Viruses (ICTV) [17]. At present, ICTV has accepted four ascovirus species based on multiple biological features. These species include *Spodoptera frugiperda ascovirus 1a* (SfAV-1a), *Trichoplusia ni ascovirus 2a* (TnAV-2a), *Heliothis virescens ascovirus 3a* (HvAV-3a) and *Diadromus pulchellus ascovirus 4a* (DpAV-4a)

The sequence reported in this paper has been deposited in GenBank/NCBI with the accession number, EF034075.

* Permanent address: AGERI, Agricultural Research Center, Department of Microbial Molecular Biology, 9 Gamaa Street, Giza 12619, Egypt.

** Current address: Entomology Department, University of Georgia, 420 Bio. Science Bldg, Athens, GA 30602, U.S.A.

*** Current address: The Centers for Disease Control and Prevention, Molecular Virology and Vaccine Branch, Influenza Division, 1600 Clifton Road, Atlanta, GA 30333, U.S.A. and School of Biology, Georgia Institute of Technology, Atlanta, GA 30332, U.S.A.

Correspondence: Xiao-Wen Cheng, Department of Microbiology, Miami University, 32 Pearson Hall, Oxford, OH 45056, U.S.A.
e-mail: Chengx@muohio.edu

[17]. Four other ascoviruses, including Spodoptera exigua ascovirus 5a (SeAV-5a), are considered members of tentative species [17]. However, SeAV-5a was recently suggested to be a variant of HvAV-3 because SeAV-5a and HvAV-3 could be cross-hybridized at high-stringency conditions [12].

Ascoviruses have a double-stranded circular genome with sizes ranging from 116 to 185 kb [3, 7, 9, 17]. Three ascovirus genomes have been sequenced recently [3, 5, 36]. Within the ascovirus genome, one open reading frame (ORF) encodes a virion structural protein, the major capsid protein (MCP) of about 50 kDa that is common to all the ascoviruses [18]. The *mcp* gene has been used in phylogenetic analyses to determine the relationship among different species within the family *Ascoviridae* and with other virus families such as *Iridoviridae* [12, 30, 40]. The ascoviruses have been suggested to have evolved from an iridovirus based on phylogenetic analyses using *mcp* and other genes, as well as the fact that many of the proteins share sequence homology between ascovirus and iridovirus [30]. However, based on the numbers of shared homologous proteins among iridovirus, ascovirus and baculovirus, and molecular phylogenetic analysis using viral DNA polymerase as well as biological and morphological characteristics, a progressive evolutionary lineage of baculovirus-ascovirus-iridovirus has been suggested [11]. Iridovirus replicates first in the nucleus, and early gene transcription also occurs in the nucleus, but there is a second phase of replication of the genome and late transcription in the cytoplasm [37]. Ascovirus replication has not been well studied but it shows similarities to that of iridoviruses [9, 16, 37]. Iridoviruses are not enclosed by membrane-bound vesicles. They appear as either naked (i.e., non-enveloped) particles or as enveloped particles that acquire a membrane by budding from the plasma membrane. There are two types of ascovirus virions: one type is enclosed in membrane-bound vesicles within the infected cells; the other type is budded out of the cells [2, 11, 37]. The membrane-bound vesicles of ascoviruses are formed by a process of partitioning of the cellular membrane, which in the case of SfAV-1a has been shown to be induced by a virus-encoded caspase gene [6]. Iridoviruses first use host RNA polymerase II for early gene transcription and later may use viral-encoded DNA-dependent RNA polymerase to transcribe other genes [19]. There have also been suggestions that genome replication and gene transcription strategies are conserved among closely related virus groups during evolution [32]. Therefore, it becomes interesting to examine if ascovirus and iridovirus share similar transcription initiation and termination strategies. This may shed light on how gene transcription is related to viral evolution. In this study, the SeAV-5a *mcp* gene was analyzed by transcription initiation and termination site determination.

Materials and methods

Cells and viruses

The insect cell line Sf21 was a culture maintained at 27 °C in Grace's medium supplemented with 10% fetal bovine serum. SeAV-5a was initially collected from haemolymph of SeAV-5a-infected *S. exigua* larvae and used to infect Sf21 cells [9, 12].

Cloning and sequencing

A SeAV-5a *Bam*HI restriction library [10] was sequenced using forward and reverse vector primers and gene-specific primers. A clone containing a 5.1-kb *Bam*HI fragment (pSKBam5.1) was found to contain a MCP homologue to other ascoviruses by a GenBank search.

Northern analysis

The virus was first titered by the endpoint dilution method. When cytopathic effect was evident (cells infected by SeAV-5a) at day 4 postinfection (p.i.), the wells with virus-infected cells were counted to calculate $TCID_{50}$ [31]. Sf21 cells (4.4×10^6 cells/75-cm^2 flask) were infected with SeAV-5a at a multiplicity of infection (MOI) of 10 $TCID_{50}$ for 1 h following the procedure of O'Reilly et al. (1992). Cells were harvested every 12 h up to 72 h. SeAV-5a-infected cells were processed for total RNA extraction [13]. Total RNA (5 µg) was analyzed with a RNA size marker (Promega) by electrophoresis on a 1% denaturing agarose gel to estimate the sizes of transcripts. RNAs thus separated were transferred onto a nylon membrane. The blot containing total RNA was hybridized to a SeAV-5a *mcp* ORF PCR fragment labeled with ^{32}P by the random primer method for 19 h. Following two stringency washings (15 min in 0.1× SSC containing 0.1% SDS at 65 °C), the blot was autoradiographied.

Table 1. A list of primers used in the transcriptional analyses of the SeAV-5a *mcp* gene

Primer names	Primer sequences
oligo (dT) 3′ RACE adapter primer*	5′-GAG CAC AGA ATT AAT ACG ACT CAC TAT AG GT_{12}VN-3′
3′ RACE outer reverse primer*	5′-GCT GAT GGC GAT GAA TGA ACA CTG-3′
MCP-F	5′-GCA ACA CCT CCT GAG ATT AC-3′
MCP-R1	5′-CAA GTC AAA CGA TTA ATT GAA ATC GC-3′
MCP-R2	5′-GTC GCC AAT ACC GTG TAT TAC-3′
MCP-115	5′-CGA GGC GTT GAG GAA TTC AGC GGA G-3′
p50ER1	5′-GTC CGG TCC GTA GAT ATA AC-3′
polh-F	5′-CCC AGA TCT ATG CCG GAT TAT TCA TA-3′
polh-R1	5′-GAT AAC GGC ACC TAA AT-3′
polh-R6	5′-ACG ATC GAT GAA CTG TTC GAA CGA G-3′
SfactinF	5′-ACG ATA TGG AGA AGA TCT GGC ACC-3′
Sfactin264R	5′-CCT CGT AGA TGG GCA CCG TGT GGG-3′
H4CE-F	5′-CGT GGA AAG GGA GGA AAA GG-3′
H4CE-R	5′-ACG TCC ATG GCG GTA ACG GTC TT-3′

* Primers from Ambion Inc.

Viral replication inhibition analysis

To determine the time frame of gene transcription of the *mcp* gene (early or late), antibiotic treatment of the cells infected by SeAV-5a was performed. Sf21 cells were infected as described above. The inoculum was removed and replaced with fresh cell growth medium containing aphidicolin (APH) at 5 μg/ml in DMSO to inhibit viral DNA replication [15, 22]. The well-studied baculovirus Autographa californica multiple nucleopolyhedrovirus (AcMNPV) was used as a reference. AcMNPV was used to infect Sf21 cells at an MOI of 10 $TCID_{50}$/cell. The treated cells were incubated at 27 °C. The controls were cells infected by either SeAV-5a or AcMNPV without APH but with DMSO. Cells were harvested for RNA extraction at 24 h p.i. [13]. RT-PCR was used to detect the effect of APH on transcription of the *mcp* gene by comparing with the effects on the well-defined late polyhedrin (*polh*) gene of AcMNPV. Total RNA (1 μg) from Sf21 cells infected either by SeAV-5a or AcMNPV at 24 h p.i. were first treated with DNase to remove contaminant DNA following recommended procedures (Promega). The DNA-free RNA was used as templates to anneal to an oligo (dT) 3′ RACE adapter primer (Table 1) at 25 °C for 10 min, and the annealed oligo (dT) primer was extended by M-MuLV reverse transcriptase (NEB) at 42 °C for 60 min to synthesize cDNA. Equal amounts of cDNA were used as template for PCR with primer pairs for the *mcp* gene transcripts (MCP-F and MCP-R1) with an anticipated product of 670 bp (Table 1). The primer pairs used for the *polh* gene transcripts were polh-F and polh-R6, with an expected product of 600 bp (Table 1). A host cellular *actin* gene (GenBank Acc. No AF548015) was targeted by a pair of *actin* primers for amplification to serve as an internal control. The *actin* primer pairs were SfactinF and Sfactin264R, which yield an expected 264-bp PCR product (Table 1). The RT-PCR was repeated three times starting from cell infection. RT-PCR products were resolved by agarose gel electrophoresis. The densities of RT-PCR products were measured by densitometry (Alphaimager version 5.1). The effects of APH on transcription of the *mcp* and *polh* genes, expressed as differences in RT-PCR product yields, were statistically analyzed by the *t*-test.

5′ Primer extension

Sf21 cells were infected with SeAV-5a as described above. In the mock infection, cells were treated similarly to the viral infection procedure, but viruses were omitted. Treated cells were incubated at 27 °C for 24 h. Subsequently, cells in the viral-infection and mock-infection cultures were harvested for total RNA extraction [13]. Total RNA (40 μg) from infected cells and mock-infected cells were annealed to a ^{32}P-labeled primer (p50ER1, Table 1) specific for the positions at 89–108 nt counting from the translation start codon of the *mcp* gene. Primer extension was carried out on the primer-template RNA duplex by using AMV in a primer-extension kit following the recommended procedure from the kit supplier (Promega). The ^{32}P-labeled primer p50ER1 was also used in a manual sequencing reaction with plasmid DNA (pSKBam5.1) to locate the transcription start site. A ^{32}P-end-labeled ϕX174 *Hin*fI DNA was used as a size marker. Primer extension products were analyzed on an 8% denaturing acrylamide gel followed by autoradiography.

3′ End mapping and polyadenylation analysis

The rapid amplification of cDNA ends (3′ RACE) method was used to map the 3′ ends of transcripts. Total RNA (1 μg) from Sf21 cells infected by SeAV-5a at 24 h p.i. for the

Northern analysis was used as template to anneal to an oligo (dT) 3′ RACE adapter primer as described above for viral replication inhibition analysis. The cDNA was used as a template for PCR with *mcp*-gene-specific forward primer (MCP-115) and 3′ RACE outer reverse primer (Table 1). The *S. frugiperda* cellular *actin* gene (AF548015) forward primer (SfactinF and 3′ RACE outer reverse primer, Table 1) were used to amplify DNA using total cellular cDNA as templates in a separate tube as a positive control for poly(A) tail detection. The negative control in the PCR amplification included everything that was present in the *mcp* gene amplification except cDNA templates. The amplified DNA was separated on a 0.9% agarose gel by electrophoresis with a DNA size marker to determine the sizes of the PCR products. PCR products were cloned into the pGEM-T Easy vector (Promega). The plasmid DNA was extracted to be used in sequencing the inserts using M13 primers.

Oligo (dT) cellulose binding analysis

To confirm the presence of poly(A) tails on SeAV-5a *mcp* transcripts, an oligo [dT] cellulose binding assay was performed. Total RNA (5 µg) harvested at 24 h p.i. from SeAV-5a-infected Sf21 cells were first treated with DNase according to the recommended protocol (Promega). The DNA-free RNA was allowed to bind to oligo (dT) cellulose (Type 3, Collaborative Research Inc.) in a binding buffer (1 M NaCl, 1 mM EDTA and 20 mM Tris, pH 8.0) for 1 h at 4 °C and washed with a washing buffer (0.3 M NaCl and 20 mM Tris, pH 8.0) in a column following the procedure recommended by the manufacturer (Collaborative Research Inc.). The RNA was eluted in water. Fractions from binding, washing and elution were collected and precipitated by centrifugation with the aid of polyacryl carrier (Molecular Research Center Inc., Ohio, U.S.A.). The precipitated RNA was dissolved in 10 µl of nuclease-free water. Since histone gene transcripts of metazoans including *Caenorhabiditis elegans* and insects contain the stem-loop structure at the 3′ terminus without a poly(A) tail, *S. frugiperda* (Sf-21 cells) H4 transcripts were targeted as a negative control in the RT-PCR analysis [21].

The affinity of RNA to oligo (dT) cellulose was analyzed using a Promega Access RT-PCR system. RNA templates (1 µl) from different fractions (binding, washing and elution) were used in RT-PCR with primer pairs for *mcp* and H4 genes in the same reaction tubes to eliminate potential pipetting errors. MCP gene primer pairs were MCP-F and MCP-R1 as mentioned above. The *C. elegans* H4 gene (NM073065) sequence was retrieved from GenBank, and a pair of primers (H4CE-F/ H4CE-R) was designed to amplify an expected PCR product of 251 bp (Table 1). Two controls were used in this analysis. One control contained everything that was present in the standard RT-PCR but without AMV and the other control contained everything for RT-PCR but without RNA templates. The RT-PCR reaction was repeated four times and the amplified products were resolved by agarose gel electrophoresis. Densities of the DNA fragments stained by ethidium bromide were quantified by densitometry (Alphaimager version 5.1). Affinities of mRNA to the oligo (dT) were calculated by dividing the densities of the eluted RT-PCR products by of the bound products for both the amplified *mcp* and H4 gene transcripts. The differences of mRNA affinities to oligo (dT) were statistically analyzed by the *t*-test procedure.

Transcription control region analysis

Sequences 100 bp upstream of the translational start sites of the SeAV-5a and other ascovirus and iridovirus MCP transcripts were aligned using LASERGENE (DNASTAR). The alignment files were entered into the GeneDoc program to perform a manual alignment [25]. Conserved motifs were identified by the GeneDoc program. The putative 3′ transcription termination regions of the *mcp* genes from ascoviruses and iridoviruses as well as a previously studied immediate-early frog virus 3 (FV3, iridovirus) gene were first searched for the eukaryotic polyadenylation signal sequence AATAAA by LASERGENE and then searched for transcribed RNA secondary structures such as stem-loop/ hairpins using the computer program Rnall [35].

RT-PCR analysis of transcription termination

To determine if transcription runs through the predicted stem-loop structure of the *mcp* mRNA, two reverse primers were used with the forward primer MCP-F. One reverse primer, MCP-R1, was located upstream of the hairpin structure, whereas the reverse primer MCP-R2 was located immediately after the termination site (nt 38 from the stop codon TAA) on the genomic DNA sequence (Table 1). The primer pairs (MCP-F/MCP-R1 and MCP-F/MCP-R2) were used in an RT-PCR containing total RNA from Sf21 cells infected by SeAV-5a (24 h p.i.) with the Access RT-PCR reagents following conditions recommended by the manufacturer (Promega). The positive control for the RT-PCR was a reaction containing the plasmid pSKBam5.1 as template. The negative control for the reaction in the RT-PCR contained no template. The amplification products were analyzed by agarose gel electrophoresis.

Results

Northern analysis

To understand the temporal transcription pattern of the *mcp* gene in insect cells, we carried out northern hybridization studies. When a ^{32}P-labeled *mcp* gene probe was used to hybridize to the total RNA from SeAV-5a-infected Sf21 cells on the blot,

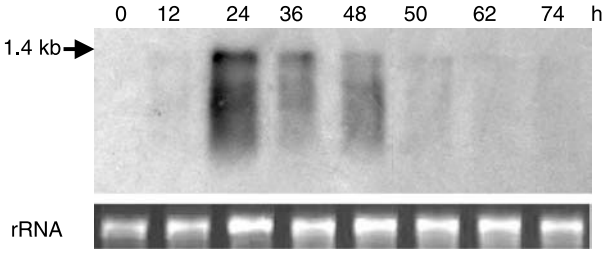

Fig. 1. Northern analysis of SeAV-5a *mcp* gene transcription in Sf21 cells. Total RNAs from different infection times were separated in a 1% agarose denaturing gel and transferred to a nylon membrane, followed by probing with a ^{32}P-labeled SeAV-5a *mcp* gene. rRNA was used as a sample loading control. The *arrow* points to the 1400-nt *mcp* gene transcript

an approximately 1.4-kb *mcp* gene mRNA transcript, which includes the coding sequence or open reading frame (ORF) of 1368 nts, was first detected at 12 h p.i. as a very faint band. The *mcp* gene transcription reached its peak at 24 h p.i., then tapered off. Smaller RNA fragments (about 500 nts in length) also hybridized to the probe, but this might represent degraded *mcp* transcripts during sample preparation. No hybridization signal was detected at time 0, which in essence was the negative control in the Northern analysis (Fig. 1).

Viral replicaton inhibition analysis

RT-PCR using *mcp* gene primer pairs (MCP-F/MCP-R1, Fig. 2A) amplified an expected 668-bp product using RNA from cells infected by SeAV-5a, either treated with aphidicolin or not treated. No PCR product was seen when the reverse transcriptase was omitted. This suggested that the RT-PCR product was generated from *mcp* gene transcripts (Fig. 2B). Similarly, *polh* primer pairs amplified an expected 600-bp product from the RNA template isolated from Sf21 cells infected by AcMNPV. In both viral infections (SeAV-5a and AcMNPV) in Sf21 cells after aphidicolin treatment, reduction of *mcp* gene and *polh* gene transcripts was observed (Fig. 2B and C). We also performed real-time quantitative PCR analyses, and similar significant reductions in transcript levels were detected for *mcp* and *polh* genes with aphidicolin treatment (data not shown). No reduction in transcription of the host cellular *actin* gene was detected (Fig. 2B and C). This suggested that the reduction of *mcp* gene transcription after applying aphidicolin was due to the effects of the antibiotics on viral DNA replication and not due to the difference in the amount of template used in RT-PCR. In the aphidicolin inhibition studies on SeAV-5a viral DNA replication in Sf21 cells, a significant reduction ($p = 0.011$) of *mcp* gene transcription (6 fold) at 24 h p.i. was observed by RT-PCR analysis. The AcMNPV late-phase *polh* transcription was reduced significantly by 9 fold ($p = 0.004$) by aphidicolin inhibition (Fig. 2C). Therefore, *mcp* should be designated as a late gene of SeAV-5a.

Mapping of 5′ and 3′ ends of mcp transcripts

The transcriptional strategy of ascovirus genes has not been studied. To understand where the transcripts of *mcp* gene start, we used a primer extension procedure to map the 5′ end of the *mcp* gene transcript. Using a primer (p50ERI, Fig. 2A) that anneals to a position 89–108 nt from the translation start codon ATG, a single primer-extension product of 133 bp in length was detected by autoradiography. No obvious cDNA primer-extension product was detected when Sf21 total cellular RNA was used as a template in the primer-extension experiment (Figs. 2A and 3A). This indicated that the primer-extension product originated from viral mRNA from SeAV-5a-infected Sf21 cells. The manual sequence reading of the 5′ untranslated region (UTR) based on radioactive signals, as shown in Fig. 3A, was CGTAGTAAATAATTAAACGT ACA. However, multiple sequencing of pSKBam5.1 by automated sequencing indicated that two base pairs at positions −4 and −8 (Fig. 3B) did not show radioactive signals. A careful examination of the manual sequence in Fig. 3A suggested that there were wider gaps than the normal gaps between other resolved bases in these two positions. This might be caused by manual sequence errors. By comparing with the manual DNA sequence obtained using the same primer (p50ER1) with pSKBam5.1 as a template and automated sequencing of pSKBam5.1, the mRNA of the *mcp* gene initiated at nt posi-

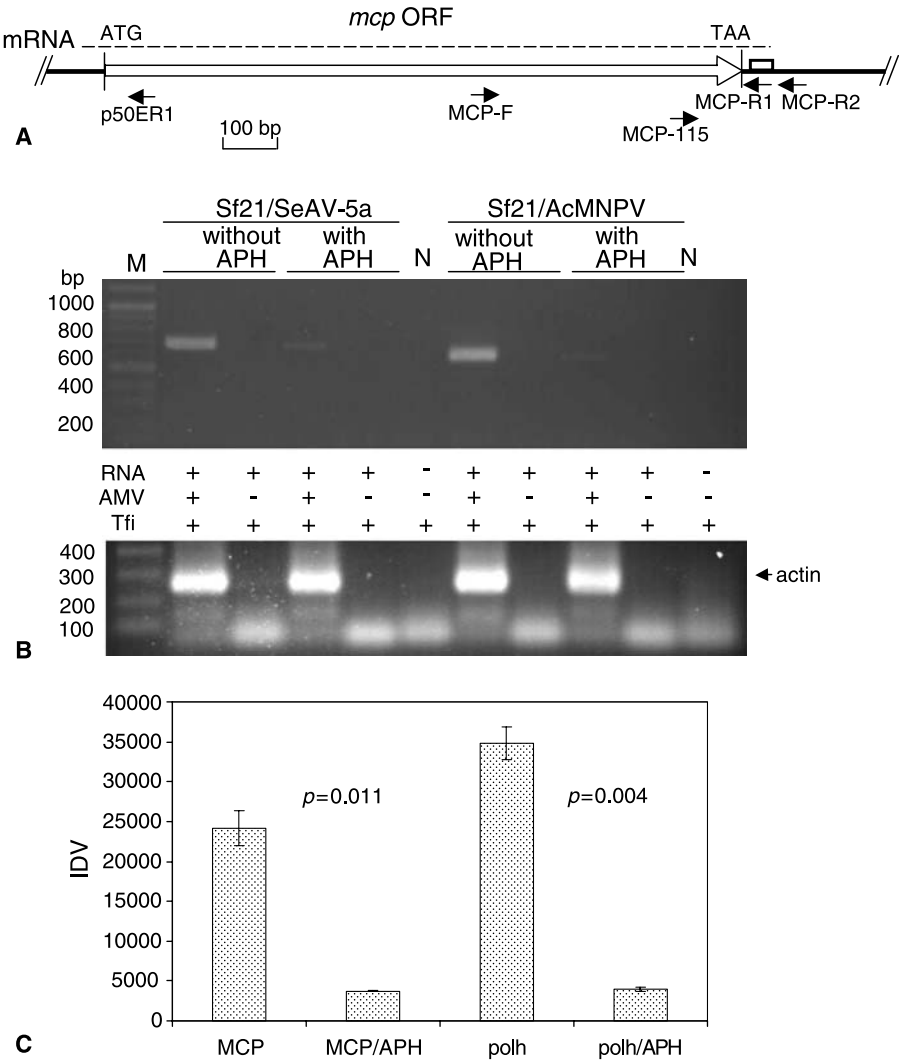

Fig. 2. Aphidicolin inhibition analyses of SeAV-5a *mcp* gene transcription. (**A**) A schematic diagram of the *mcp* gene to indicate primer positions for transcriptional analyses. The *large arrow* (⟹) represents the *mcp* orf. The *small box* (▭) indicates the predicted stem-loop structure. *Thick lines* (—) represent flanking sequences. *Double slash lines* (//) denote omitted sequences. The *mcp* mRNA is represented by a dashed line. (**B**) RT-PCR analysis of the effects of aphidicolin (APH) (5 μg/ml) on transcription of the *mcp* gene. Total RNA was extracted from Sf21 cells infected either by SeAV-5a or AcMNPV at 24 h postinfection. RT-PCR was used to detect reduction in transcription of *mcp* of SeAV-5a and the late *polh* gene of AcMNPV with *mcp* and *polh* primers. Host *actin* gene amplification by RT-PCR was used to normalize the reaction. *M* DNA size marker. *N* negative control. (**C**) Quantitative analysis of the effects of aphidicolin (APH) on the transcription of the *mcp* gene. Densities of RT-PCR products from agarose gel electrophoresis were measured by densitometry and the differences in densities between the treated (MCP/APH or polh/APH) and untreated (MCP or *polh*) samples were analyzed statistically (*t*-test). Probabilities (p) are shown for *mcp* and *polh*, respectively. *IDV* Integrated density value. *Vertical lines* on the bars represent standard error for the mean ($n = 3$)

tion −25 with reference to the A as +1 in the ATG translation start codon, with a cytosine as the first nucleotide in the transcript of the *mcp* gene (Fig. 3A and B).

In addition to the 5′ end mapping, 3′ RACE was performed to provide some insight into potential termination strategies of ascovirus gene transcription. Using cDNA synthesized from total RNA

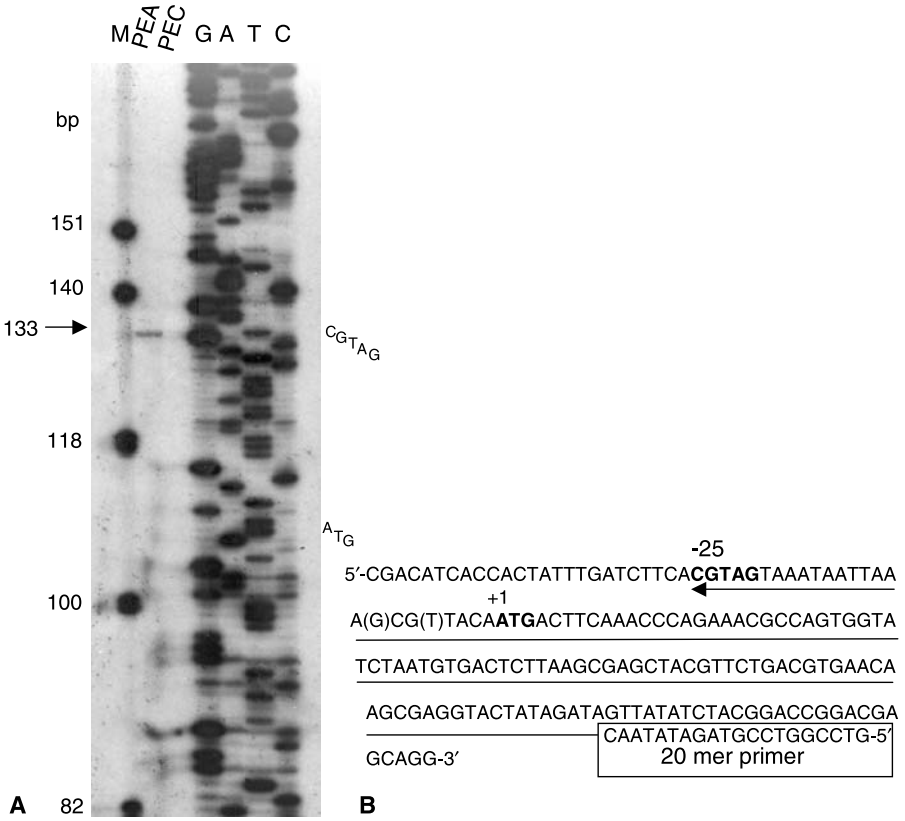

Fig. 3. Primer extension analysis of the SeAV-5a *mcp* gene. (**A**) Denaturing polyacrylamide gel analysis of the primer extension product and termination of the product size with marker (M) and manual sequencing ladder using a primer extension primer and a plasmid clone (pSKBam5.1) containing the *mcp* gene in the sequencing reaction. PEA, primer extension with total RNA from ascovirus-infected cells. PEC, primer extension with total RNA from cells not infected by ascovirus (*negative control*). (**B**) A schematic representation of the 5′ end of *mcp* gene deduced from panel A and automated sequencing. Nucleotides in *parentheses* indicate sequences resolved by automated sequencing from plasmids but not from manual sequencing in panel A

from SeAV-5a-infected Sf21 cells with an oligo (dT) adapter primer (Table 1), the 3′ outer reverse primer and *mcp*-gene-specific forward primer produced a major PCR product of about 190 bp in the PCR reaction. There were no discrete PCR products in the negative control where no cDNA template was added to the reaction. A positive control using *S. frugiperda* cellular *actin* gene-specific forward primer and 3′ outer reverse primer produced a major PCR product of about 150 bp (Fig. 4). This 3′ RACE experiment suggested that SeAV-5a *mcp* gene transcripts were polyadenylated, as the oligo (dT) 3′ RACE adapter primer was able to anneal to the putative poly(A) tail of the *mcp* gene for cDNA synthesis. The SeAV-5a *mcp* gene 3′ RACE product was cloned into the pGEM-T Easy vector, and seven clones were sequenced. The sequence results indicated transcripts of the *mcp* gene more frequently ended at nt 26 (six clones) and less frequently at nt 38 (one clone) counting from the last nt of the translation stop codon (TAA) with the last nucleotide as a U (T in Fig. 6). The sequence results also confirmed that the sizes of the 3′ RACE products were about 190 bp (146–158 bp from template plus 44 bp from oligo (dT) 3′ RACE adapter). Since there were 25 nts of UTR sequence at the 5′ end of the *mcp* ORF and 24 or 38 nts of sequence at the 3′ UTR, the expected length of the transcripts was 1418 or 1431 nts, which confirmed the sizes of the transcripts of *mcp* in the Northern analysis (Fig. 1).

Further evidence from the oligo (dT) cellulose binding experiment supported that the SeAV-5a

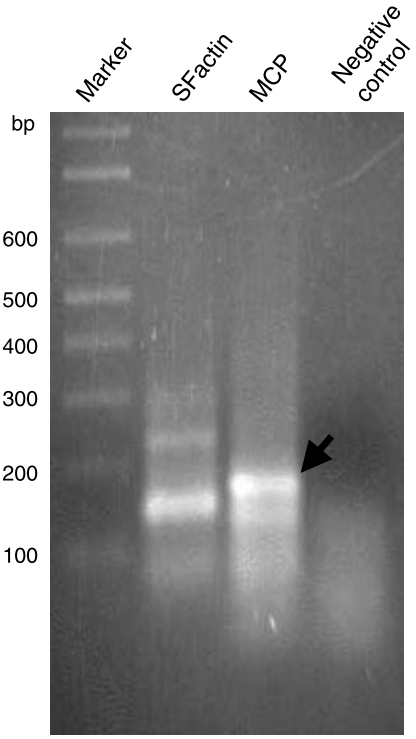

Fig. 4. Analysis of the 3′ end termination of *mcp* gene transcripts by rapid amplification cDNA ends (3′ RACE). The *mcp*-gene-specific forward primer and 3′ RACE outer primer (*reverse*) were used to amplify products using cDNA templates from Sf21 cells infected by SeAV-5a (MCP). *S. frugiperda actin* gene-specific primer (*forward*) and 3′ RACE outer primer (*reverse*) were used to amplify products using cDNA templates from Sf21 cells infected by SeAV-5a (SFactin, positive control). A reaction that contained everything in the MCP reaction except cDNA templates was used as a negative control. The *arrow* points to the *mcp* gene 3′RACE product

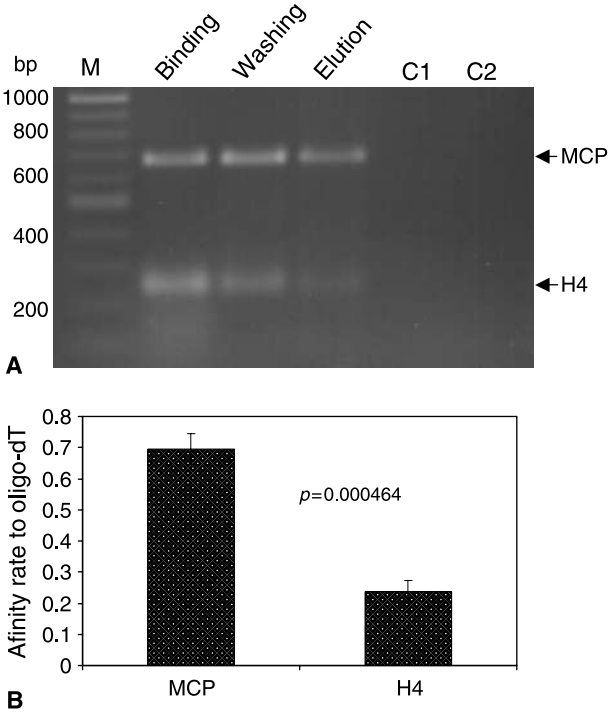

Fig. 5. Affinity analysis of the *mcp* gene mRNA to oligo (dT) cellulose. (**A**) Total RNA isolated from Sf21 cells infected with SeAV-5a was allowed to bind to the oligo (dT) cellulose, followed by stringency washing and elution of RNA. RNA in the binding, washing and elution fractions were precipitated and used to amplify *mcp* and *S. frugiperda* H4 gene mRNA by RT-PCR. M. DNA size marker. C1, RT-PCR without AMV. C2, RT-PCR without template. (**B**) Quantitative affinity comparison of *mcp* and H4 mRNA to the oligo (dT) cellulose. Densities from *mcp* and H4 RT-PCR products were measured by densitometry. Affinity rates were calculated by dividing PCR product densities from elution by PCR product densities from binding. The affinity difference between *mcp* and H4 to oligo (dT) cellulose was statistically tested (*t*-test). *Vertical lines* on the bars represent standard error for the mean ($n = 4$)

mcp gene transcripts contain poly(A) tails. Using *mcp* primer pairs, an expected 670-bp product with similar yields was detected by RT-PCR, and no PCR product was detected when no AMV or no template was added to the amplification reactions. This suggested that the RT-PCR products from the three fractions (binding, washing and elution) came from templates of *mcp* gene mRNA. There was a steady decrease in RT-PCR yields for the H4 gene transcripts of Sf21 (Fig. 5A). Quantification of the PCR products showed that *mcp* mRNA had a significantly higher affinity to the oligo (dT) cellulose than the Sf21 host H4 mRNA, which contains no poly(A) tail ($p = 0.000464$) (Fig. 5B). Therefore, it is highly likely that the SeAV-5a *mcp* gene mRNA has a poly(A) tail that can bind to the oligo (dT) cellulose.

Transcription control region analysis

To build a consensus of the 5′ and 3′ transcription control regions of *mcp* gene transcripts, available *mcp* genes from other ascoviruses and CIV were used for alignment. Alignment of the 5′ transcription control regions of the *mcp* transcript among

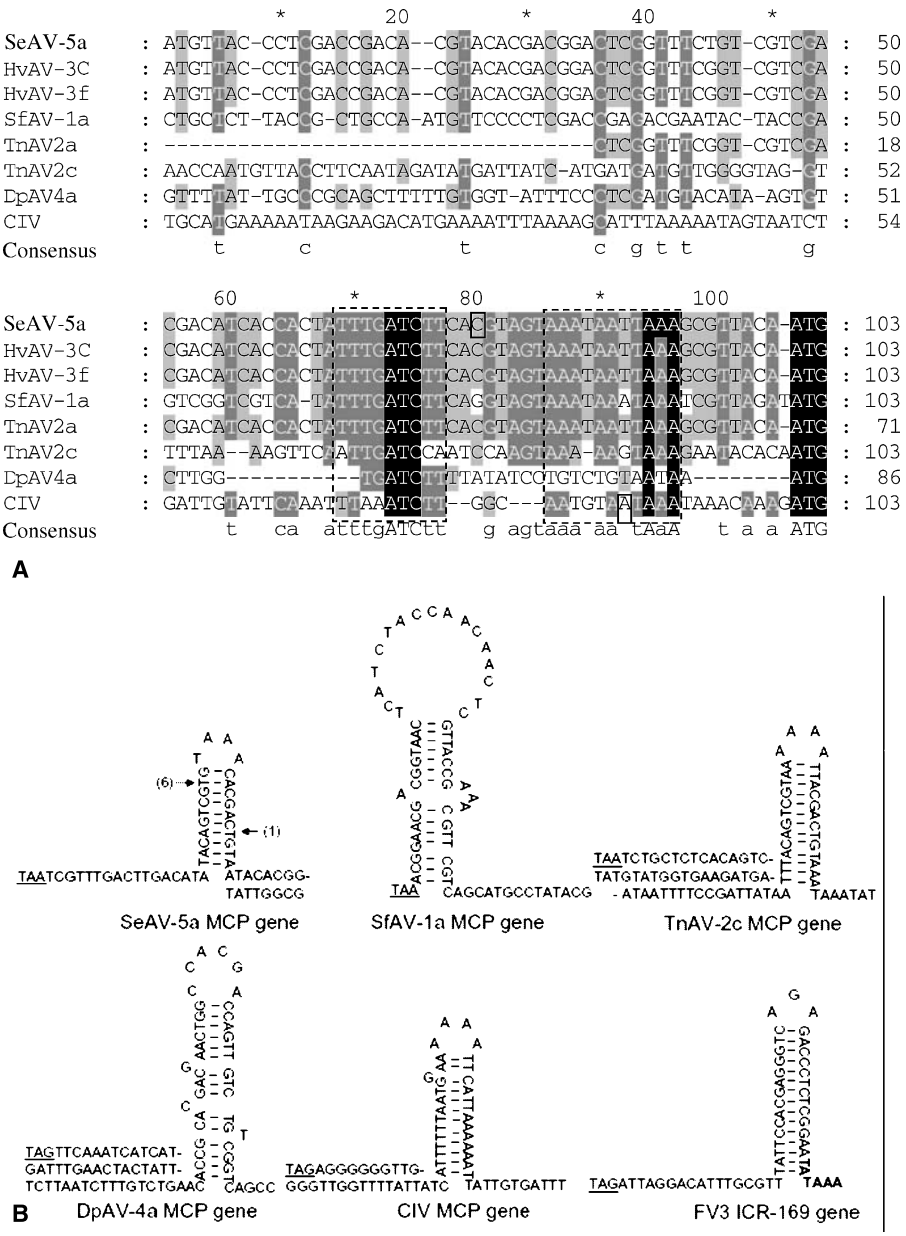

Fig. 6. Sequence analysis of putative regulatory regions of the *mcp* gene of ascoviruses and CIV as well as other iridovirus genes. (**A**) Identification of conserved motifs in the *mcp* gene upstream regions. *Dashed lines* indicate absence of nucleotides. Nucleotides in *solid-line* boxes indicate transcription start sites for SeAV-5a and CIV *mcp* genes, respectively. *Dashed boxes* indicate conserved motifs in the regulatory regions of the *mcp* gene between ascovirus and CIV. (**B**) Gene downstream sequence analysis. Downstream sequences of the *mcp* gene of ascoviruses and CIV as well as frog virus 3 (FV3) ICR-169 gene (iridovirus) showing stem-loop structures. Sequences start with the translation stop codon TAA or TAG (*underlined*). Arrows point to the last nucleotides in the SeAV-5a *mcp* transcripts. Numbers in parentheses indicate the number of clones sequenced. Nucleotides of the FV3 ICR-169 gene in *bold* indicate the heterogeneous regions of termination [38]. SeAV-5a, Spodoptera exigua ascovirus 5a (EF034075). HvAV-3c and -3f, Heliothis virescens ascovirus 3c and -3f (AJ312704, AF419098), DpAV-4a, Diadromus pulchellus ascovirus 4a (AJ312705). SfAV-1a, Spodoptera frugiperda ascovirus 1a (AJ312690), TnAV-2a and -2c, Trichoplusia ni ascovirus 2a and 2c (AJ312707, DQ517337), CIV, Chilo iridescent virus (AF303741), frog virus 3 ICR-169 gene (NC_005946)

ascoviruses revealed that the eukaryotic class II promoter consensus sequence TATAAA (TATA box) was not present in the upstream region of the SeAV-5a *mcp* gene. However, a TATA-box-like motif (TAATTAAA) was found downstream of the transcription initiation site (Fig. 6A). A downstream ORF (*p27*) showed a similar 5′ transcription control region motif compared with the *mcp* 5′ transcription control regions (data not shown). An alignment with 5′ transcription control regions of other available *mcp* sequences revealed at least two highly conserved sequence elements in this region within 40 nts upstream of the translation initiation codon ATG among ascoviruses and CIV. One of the consensus elements, located downstream of the transcription initiation site, was GTAGTAAATAATT AAA. The other element was upstream of the transcription initiation site (ATTTGATCTT). In both ascovirus and CIV, the transcriptional start sites were preceded by AT-rich regions (Fig. 6A). The SeAV-5a, HvAV-3c, HvAV-3f, SfAV-1a and TnAV-2a showed more sequence similarity with each other in the transcription control regions than with TnAV-2c, DpAV-4a and CIV.

A search for the eukaryotic polyadenylation consensus signal sequence AATAAA near the 3′ end region of the SeAV-5a *mcp* ORF revealed no such sequence between the translation stop codon TAA and transcription termination site. There is a possible AATAAA variant GTAAA sequence seven nts upstream of the transcription termination site, a TAATA sequence at one nt downstream of the transcription termination site, and a CAAAAA hexamer at 21 nts downstream of the transcription site. To our surprise, a short complete inverted repeat of 10 nts was found, and it formed a stem-loop or a typical hairpin structure. The stem-loop was formed from nts 21 to 44 counting from the last nucleotide of TAA. The stem-loop structure contains 10 complete base pairs in the stem and four nucleotides in the loop (Fig. 6B). A search of other *mcp* gene sequences for this stem-loop structure revealed that it was present near the 3′ end region of the *mcp* genes. However, the length of the stem, the stem base pairings, loop length and nucleotide composition among different stem-loop structures were the same among some but different among others. The AT:GC ratio is 50% in the stem-loop in the *mcp* 3′ end of SeAV-5a (Fig. 6B). Both TnAV-2c and CIV *mcp* 3′ stem-loops were also formed by complete inverted repeats of 14 nucleotides rich in AT, 71% and 86%, respectively; both had four A nucleotides in the loop (Fig. 6B). SfAV-1a and DpAV-4a *mcp* genes had incomplete inverted repeats of about 17 nucleotides, with lower AT content in the stem, about 50% for both (Fig. 6B).

Transcription termination

A discrete RT-PCR product band of *mcp* transcripts was resolved by agarose gel electrophoresis (Fig. 4), but this could not rule out the possibility that transcription ran through the predicted stem-loop structure from the DNA sequences. When a reverse primer (MCP-R2, Fig. 2A) located immediately downstream of the termination site (nt 38) in the stem-loop structure was used together with the forward primer (MCP-F) in a RT-PCR, no amplified product was detectable by agarose gel electrophoresis. However, the primer pair MCP-F/

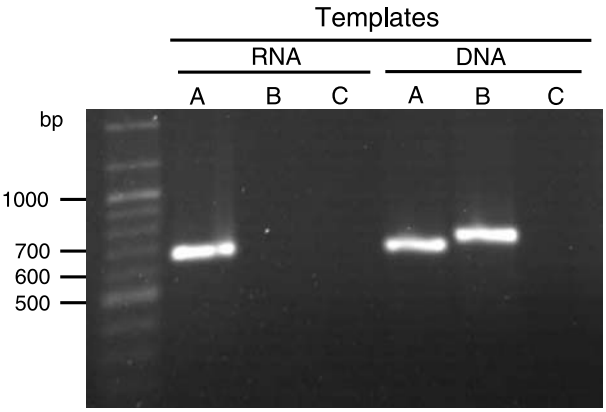

Fig. 7. RT-PCR analysis of SeAV-5a *mcp* gene transcription termination. A forward primer (MCP-F) from the middle region of the *mcp* gene was paired with either a reverse primer (MCP-R1) from upstream of the predicted stem-loop structure (Figs. 2A and 6B) or a reverse primer immediately downstream of the stem-loop structure in a RT-PCR with RNA isolated from SeAV-5a-infected Sf21 cells (24 h p.i.). In the positive control, plasmid pSKBam5.1 DNA was used as a template for the amplification. *A* Primer pair MCP-F/MCP-R1. *B* primer pair MCP-F/MCP-R2. *C* Negative control with primer pair MCP-F/MCP-R1 but without template

MCP-R1 (Fig. 2A) produced an expected 670-bp RT-PCR product from a RNA template. The primer pair MCP-F/MCP-R2 produced a 715-bp DNA product, which is 45 bp larger than the product by MCP-F/MCP-R1 primer pairs from DNA template (pSKBam5.1) (Fig. 7). This confirmed that the transcription of the *mcp* gene terminated upstream of the MCP-R2 sequence, which is immediately downstream of the predicted stem-loop structure.

Discussion

In this study, we mapped the 5′ and 3′ ends of the *mcp* gene transcripts of SeAV-5a. To the best of our knowledge, this is the first study to map the transcription initiation site of an ascovirus gene and the first time to demonstrate that the transcripts of the *mcp* gene of SeAV-5a are polyadenylated when the viral morphogenesis takes place in the cytoplasm of infected cells. We show for the first time that the *mcp* genes of ascoviruses may use a stem-loop structure for possible transcription termination.

The *mcp* gene of CIV is classified as a late gene which is transcribed after DNA replication [15, 24]. Systematic classification of ascovirus genes based on temporal transcription after viral infection has not yet been done. However, the transcription of *mcp* genes of SeAV-5a starts at 12 h postinfection and peaks at 24 h in cell culture, which may suggest it to be a late gene (Fig. 1). By comparing to the effects of aphidicolin on late *polh* gene transcription suppression of AcMNPV, aphidicolin can significantly reduce the levels of transcripts of the *mcp* gene of SeAV-5a (Fig. 2). Therefore, the *mcp* gene of ascovirus is a late gene. The level of reduction of SeAV-5a *mcp* transcripts after aphidicolin treatment was slightly lower than that of AcMNPV *polh* (Fig. 2). This could be due to differences in sensitivity of the DNA polymerases in AcMNPV and SeAV-5a. It could also be due to the primer pairs used for the two genes (*mcp* and *polh* genes). A similar reduction of the late *mcp* gene transcripts of CIV by aphidicolin inhibition has been observed [15].

The sequences of the coding regions of the *mcp* genes from ascoviruses and CIV predicted that ascoviruses and iridoviruses are closely related [11, 30]. It has been suggested that the transcription strategy is maintained during the viral evolution process in closely related viruses [32]. Our transcription analyses of SeAV-5a support this suggestion by showing similarities in the 5′ and 3′ transcription regulatory regions of the *mcp* genes in the ascovirus and iridovirus (Fig. 6).

The putative 5′ regulatory region of SeAV-5a *mcp* gene transcripts does not show high similarity to typical eukaryotic gene promoters with a CCAAT box and GC box (GGGCGG and CCG CCC) upstream of a TATA box (consensus sequence TATAAA). The putative 5′ regulatory region of the *mcp* gene of SeAV-5a showed similarity to that of CIV. Both contain the conserved motif TAATTAAA, a TATA box-like motif. However, a conserved eukaryotic promoter motif, the CAAT box, is not found within 300 bp upstream of the transcription start site (Fig. 6A). Another conserved motif is ATCTT, which is located upstream of the TAATTAAA motif and shared by the two groups (Fig. 6A). The transcription initiation site is different between the SeAV-5a *mcp* gene and CIV *mcp* gene. The SeAV-5a *mcp* gene transcript starts with a C as the start site, which is 25 nts upstream of the translation start site, whereas the CIV *mcp* gene transcript starts with an A, which is 14 nts upstream of the translation start site [24]. The SeAV-5a *mcp* gene transcripts start between the two conserved motifs (Fig. 6A), whereas the transcription start site of the CIV *mcp* gene is within the second motif (25, Fig. 6A). This suggests that the transcription factors that recruit RNA polymerases to the promoter region of the two viruses may have differences in the protein structures which interact with the promoter region of the *mcp* gene. The transcription start site of the SeAV-5a *mcp* gene resembles that of the DNA polymerase gene of CIV, with the first nucleotide being C, which is 35 nts upstream of the translation start site [22]. The exact transcription start site may depend on the polymerase and the associated transcription initiation factors.

Host cells use RNA polymerase II to synthesize mRNA with poly(A) tails. The addition of the poly(A) tail is catalyzed by poly-A polymerase

(PAP) which is recruited to the cleaved 3′ end by other RNA processing factors [23, 28]. Two independent approaches, using 3′ RACE and oligo (dT) cellulose binding affinity assay, suggest that the *mcp* gene of SeAV-5a is polyadenylated, forming a poly(A) tail (Figs. 4 and 5). The experiment using 3′ RACE to detect poly(A) tails is sequence specific, requiring a stretch of As to anneal to the oligo (dT) primer. Furthermore, the amplified products can be cloned and sequenced to verify where the termination occurs. It can, therefore, provide strong evidence of the presence of poly(A) tails. Oligo (dT) cellulose may bind to stretches of As that may be present within the ORF or 5′ UTR. Conditions of stringency washing may also affect the yield of poly(A)-tailed mRNA in the elution. Therefore, the oligo (dT) cellulose binding assay requires quantitative analysis. We did not optimize the washing conditions for the oligo (dT) cellulose binding assay, but the conditions we used for both the *mcp* gene and H4 gene mRNA were the same, and significant differences in affinities for the oligo (dT) cellulose were detected between the two genes examined. No PAP gene has been identified in ascovirus genomes [3, 5, 31]. It is likely SeAV-5a has no PAP gene in the genome. Therefore, the ascovirus gene may have been polyadenylated by the host PAP. No poly(A) tails of late gene transcripts were detected in the cytoplasm of cells infected by ascovirus-related iridovirus [39]. This is probably due to the fact that replication of iridovirus does not break down the nuclear envelope [37].

Host mRNAs are transcribed by RNA polymerase II, and transcription termination is carried out by a cleavage/polyadenylation mechanism. This process is triggered by a well-conserved specific polyadenylation signal sequence (AATAAA) about 10–30 nt upstream of the cleavage site [34]. No actual polyadenylation signal sequence can be found between the translation stop codon and transcription termination site in the 3′ UTR of the SeAV-5a *mcp* gene. A possible variant polyadenylation signal sequence GTAAA in the 3′ UTR is not within 11–30 nt of where the polyadenylation starts. Other possible signals downstream of the 3′ termination site are unlikely to be involved in polyadenylation because they are not in the right place. This suggests that ascovirus late genes are not terminated by the cleavage/polyadenylation mechanism. Other cytoplasmic poxvirus and Africa swine fever virus (ASFV) may also not use the host nuclear cleavage/polyadenylation system to process the 3′ ends of the transcripts as they replicate in the cytoplasm with an intact nucleus.

ASFV late mRNA termination is within the conserved 7U motif [1, 26]. In contrast, the poxvirus late genes lack defined 3′ ends that specify the termination, but they can be polyadenylated by the viral-encoded PAP [8, 14, 20]. Near the 3′ end region of the *mcp* ORF, a stem-loop structure can be formed, and the termination of transcripts occurred within the predicted stem-loop structure (Fig. 6B). Dyad symmetry (hairpin structure) at the 3′ termini of immediate-early and late FV3 (iridovirus) has been reported [4]. Similar regions with dyad symmetry at the 3′ end of the putative integrase gene have also been mapped and have been suggested to be involved in transcription termination in FV3 [27]. Immediate-early FV3 ICR-169 gene transcripts were mapped to terminate within a third AT-rich region about 50 to 60 bp downstream of the translation stop codon [38]. Analyses using the computer program Rnall [35] predicted that the termination occurred immediately after a stem-loop structure (Fig. 6B). The 3′ terminal region of SeAV-5a *mcp* gene transcripts from the second termination site (nt 38) can still form a stem-loop structure with seven base pairings in the stem portion of the structure (Fig. 6B). If this stem-loop structure of the *mcp* transcript is responsible for the termination, the first and the more frequent termination site (nt 26) might be produced by nuclease cleavage before polyadenylation occurs. The stem-loop structure and termination position of the SeAV-5a *mcp* gene and the FV3 INT gene as well as the FV3 ICR-169 gene transcript is similar to the bacterial intrinsic transcription termination hairpin structure, which counts for about 50% gene transcription termination. However, the stem-loop structure of *mcp* transcripts is not followed by a stretch of A:U base pairs that exemplify the bacterial hairpin [33]. Many of the SfAV-1a genes showed inverted repeats, but hairpin struc-

tures and 3′ ends of transcripts were not analyzed and mapped [29]. About half of the putative genes in TnAV-2c contain strong stem-loop structure near the 3′ end regions of its 165 ORFs [36]. We have not yet tested if the stem-loop structure is actually responsible for the termination of the *mcp* gene transcripts, which may require mutagenesis of the stem portion of the structure to verify its function in termination of *mcp* gene transcripts. More ascovirus genes need to be analyzed using methods such as 3′ RACE to see if the termination is always in the stem-loop structure. Based on current knowledge of transcription termination mechanisms in different organisms, the stem-loop structures in the *mcp* gene transcripts may likely be the trigger for the RNA polymerase to fall off to terminate the transcripts. Once the transcripts terminate, the host PAP adds a stretch of adenines to the end of the transcripts to form poly(A) tails.

There are many proteins that share sequence homology between ascovirus and iridovirus, and molecular phylogenetic prediction suggested that the two groups of viruses are closely related. The similarities of conserved motifs in the 5′ transcription control regions and the stem-loop structure in the 3′ end region of the *mcp* genes between the ascoviruses and iridoviruses further support the assertion that gene transcription strategies are conserved between these two closely related groups of viruses during evolution.

Acknowledgments

We would like to thank Drs. G. R. Carner and B. M. Arif for providing assistance in the early stage of this work. Drs. Q. Li, J. Stevenson and E. Bridge are credited for discussion, comments and proofreading of the manuscript. We also thank Dr. G. Janssen for reagent sharing. Part of the financial support comes from the College of Arts and Science new faculty startup fund to XWC at Miami University.

References

1. Almazan F, Rodriguez JM, Angulo A, Vineula E, Rodrigues JF (1993) Transcriptional mapping of a later gene coding for the p12 attachment protein of African swine fever virus. J Virol 67: 553–556
2. Asgari S (2006) Replication of *Heliothis virescens* ascovirus in insect cell lines. Arch Virol 151: 1689–1699
3. Asgari S, Davis J, Wood D, Wilson P, McGrath A (2007) Sequence and organization of the *Heliothis virescens* ascovirus genome. J Gen Virol 88: 1120–1132
4. Aubertin AM, Tondre L, Tham TN (1989) Translational regulation of frog virus 3. In: Ahne W, Kurstak E (eds) Viruses of lower vertebrates. Springer-Verlag, Berlin, Heidelgerg, pp 51–59
5. Bideshi DK, Demattei MV, Rouleux-Bonnin F, Stasiak K, Tan Y, Bigot S, Bigot Y, Federici BA (2006) Genomic sequence of the *Spodoptera frugiperda* ascovirus 1a, an enveloped, double-stranded DNA insect virus that manipulates apoptosis for viral reproduction. J Virol 80: 11791–11805
6. Bideshi DK, Tan Y, Bigot Y, Federici BA (2005) A viral caspase contributes to modified apoptosis for virus transmission. Genes Dev 19: 1416–1421
7. Bigot Y, Rabouille A, Sizaret PY, Hamelin MH, Periquet G (1997) Particle and genomic characterization of a new member of the Ascoviridae, *Diadromus pulchellus* ascovirus. J Gen Virol 78: 1139–1147
8. Brown M, Dorson JW, Bollum FJ (1973) Terminal riboadenylate transferase: a poly A polymerase in purified vaccinia virus. J Virol 12: 203–208
9. Cheng XW, Carner GR, Arif BM (2000) A new ascovirus from *Spodoptera exigua* and its relatedness to the isolate from *Spodoptera frugiperda*. J Gen Virol 81: 3083–3092
10. Cheng XW, Henriques TR, Coppens SR, Feng Q, Retnakaran A, Krell PJ, Arif BM (2003) Strategy to screen long DNA inserts in *Escherichia coli*. Biotechniques 34(6): 1162–1164
11. Cheng XW, Wan XF, Xue JL, Moore RC (2007) Ascovirus and its evolution. Virologica Sinica 22: 137–147
12. Cheng XW, Wang L, Carner GR, Arif BM (2005) Characterization of three ascovirus isolates from cotton insects. J Invertebr Pathol 89: 193–202
13. Chomczynski P, Sacchi N (1987) Single-step method of RNA isolation by acid guanidinium thiocyanate-phenol-chloroform extraction. Anal Biochem 162: 156–159
14. Cooper JA, Wittek R, Moss B (1981) Extension of the transcriptional and translational map of the left end of the vaccinia virus genome to 21 kilobase pairs. J Virol 39: 733–745
15. D'Costa SM, Bilimoria SL (2001) Transcription and temporal cascade in *Chilo* iridescent virus infected cells. Arch Virol 146: 2165–2178
16. Federici BA (1983) Enveloped double-stranded DNA insect virus with novel structure and cytopathology. Proc Natl Acad Sci USA 80: 7664–7668
17. Federici BA, Bigot Y, Granados RR, Hamm JJ, Miller LK, Newton I, Stasiak K, Vlak JM (2005) Family Ascoviridae. In: Fauquet CM, Mayo MA, Maniloff J, Desselberger U, Ball LA (eds) Virus taxonomy. Seventh 8th Report of the International Committee on Taxonomy of Viruses, pp 261–265. Edited by van Regenmortel

MHV, Fauquet CM, Bishop DHL, Carstens EB, Estes MK, Lemon SM, Maniloff J, Mayo MA, McGeoch DJ, Pringle CR, Wickner RB. Elsevier Academic Press, San Diego, Calif, Academic Press, San Diego, pp 269–274
18. Federici BA, Govindarajan R (1990) Comparative histopathology of three ascovirus isolates in larval noctuids. J Invertebr Pathol 56: 300–311
19. Jakob NJ, Muller K, Bahr U, Darai G (2001) Analysis of the first complete DNA sequence of an invertebrate iridovirus: coding strategy of the genome of *Chilo* iridescent virus. Virology 286: 182–196
20. Mahr A, Roberts BE (1984) Arrangement of late RNAs transcribed from a 7.1 kilobase EcoRI vaccine virus DNA fragment. J Virol 49: 510–520
21. Marzluff WF (2005) Metazoan replication-dependent histone mRNAs: a distinct set of RNA polymerase II transcripts. Curr Opin Cell Biol 17: 274–280
22. Miller LK, Jewell LE, Brown D (1981) Baculovirus induction of a DNA polymerase. J Virol 40: 305–308
23. Mivnielle-Sebastia L, Keller W (1999) mRNA polyadenylation and its coupling to other RNA processing reactions and to transcription. Curr Opin Cell Biol 11: 352–357
24. Nalcacioglu R, Marks H, Vlak JM, Demirbag Z, van Oers MM (2003) Promoter analysis of the *Chilo* iridescent virus DNA polymerase and major capsid protein genes. Virology 317: 321–329
25. Nicholas KB, Nicholas HB Jr, Deerfield DW II (1997) GeneDoc: analysis and visualization of genetic variation. EMBNEW NEWS 4: 14
26. Rodriguez JM, Salas ML, Vinuela E (1996) Intermediate class of mRNAs in Africa swine fever virus. J Virol 70: 8584–8589
27. Rohozinski J, Goorha R (1992) A frog virus 3 gene codes for a protein containing the motif characteristic of the INT family of integrases. Virology 186: 693–700
28. Shatkin AJ, Manley JL (2000) The ends of the affair: capping and polyadenylation. Nat Struct Biol 7: 838–842
29. Stasiak K, Demattei MV, Federici BA, Bigot Y (2000) Phylogenetic position of the DpAV-4a ascovirus DNA polymerase among viruses with a large double-stranded DNA genome. J Gen Virol 81: 3059–3072
30. Stasiak K, Renault S, Demattei M, Bigot Y, Federici BA (2003) Evidence for the evolution of ascoviruses from iridoviruses. J Gen Virol 84: 2999–3009
31. Summers MD, Smith GE (1987) A manual of methods for baculovirus vectors and insect cell culture procedures. Texas Agricultural Experiment Station Bulletin, no. 1555
32. Villarreal LP (2005) Virus and the evolution of life. ASM press, Washington, DC
33. Von Hippel PH (1998) An integrated model of the transcription complex in elongation, termination, and editing. Science 281: 660–665
34. Wahle E, Keller W (1992) The biochemistry of 3′end cleavage and polyadenylation of messenger RNA precursors. Annu Rev Biochem 61: 419–440
35. Wan XF, Lin G, Xu D (2006) Rnall: an efficient algorithm for predicting RNA local secondary structural landscape in genomes. J Bioinform Comput Biol 4: 1015–1031
36. Wang L, Xue J, Seaborn CP, Arif BM, Cheng XW (2006) Sequence and organization of the *Trichoplusia ni* ascovirus 2c (*Ascoviridae*) genome. Virology 354: 167–177
37. Williams T, Barbosa-Solomieu V, Chinchar VG (2005) A decade of advances in iridovirus research. In: Maramorosch K, Shatkin AJ (eds) Advances in virus research, vol. 65. Elsevier Academic Press, San Diego, Calif., pp 174–248
38. Willis D, Foglesong D, Granoff A (1984) Nucleotide sequence of an immediate-early grog virus 3 gene. J Virol 53: 905–912
39. Willis D, Granoff A (1976) Macromolecular synthesis in cells infected by frog virus 3 V. The absence of polyadenylic acid in the majority of virus-specific RNA species. Virology 73: 543–547
40. Zhao K, Cui LW (2003) Molecular characterization of the major virion protein gene from the *Trichoplusia ni* ascovirus. Virus Genes 27: 93–102